

Study of Minority Carrier Diffusion Lengths in Photoactive Layers of Multijunction Solar Cells

S. A. Mintairov[^], V. M. Andreev, V. M. Emelyanov, N. A. Kalyuzhnyy, N. K. Timoshina,
M. Z. Shvarts, and V. M. Lantratov

Ioffe Physical Technical Institute, Russian Academy of Sciences, ul. Polytekhnicheskaya 26, St. Petersburg, 194021 Russia

[^]e-mail: mintairov@scell.ioffe.ru

Submitted December 30, 2009; accepted for publication January 13, 2010

Abstract—A technique for determining a minority carrier's diffusion length in photoactive III–V layers of solar cells by approximating their spectral characteristics is presented. Single-junction GaAs, Ge and multijunction GaAs/Ge, GaInP/GaAs, and GaInP/GaInAs/Ge solar cells fabricated by hydride metal–organic vapor-phase epitaxy (H-MOVPE) have been studied. The dependences of the minority carrier diffusion length on the doping level of *p*-Ge and *n*-GaAs are determined. It is shown that the parameters of solid-state diffusion of phosphorus atoms to the *p*-Ge substrate from the *n*-GaInP nucleation layer are independent of the thickness of the latter within 35–300 nm. It is found that the diffusion length of subcells of multijunction structures in Ga(In)As layers is smaller in comparison with that of single-junction structures.

DOI: 10.1134/S1063782610080233

1. INTRODUCTION

The recent development of solar power engineering is caused by the advent of more efficient thin-film polycrystalline and single-crystal III–V photoconverters [1]. However, only the use of multijunction (MJ) heterostructures based on III–V materials has made it possible to achieve solar cell (SC) efficiencies above 40% and fabricate radiation resistant structures for space applications [2–5].

MJ SCs consist of several subcell heterostructures, including a *p*–*n* junction and barrier layers. Subcells are arranged along the decrease in the band gaps of their material from the photosensitive surface to the substrate and are interconnected by growing opposite connected tunneling diodes in monolithic structures. Thus, each subcell converts only a fraction of the incident spectrum into energy, which allows a significant increase in the efficiency of the structure as a whole.

The most efficient monolithic GaInP/GaInAs/Ge MJ SCs to date are grown by hydride metal–organic vapor-phase epitaxy (H-MOVPE) on *p*-Ge substrates and feature *n*–*p* polarity. In this case, the bottom *p*–*n* junction in the substrate is formed due to solid-state diffusion of phosphorus atoms from the *n*-GaInP nucleation layer deposited on the surface. The small depth of the *p*–*n* junction in Ge during diffusion of phosphorus atoms, which provides optimum parameters of this *p*–*n* junction, generally defines the *n*–*p* polarity of the GaInP/GaInAs/Ge MJ SC. Furthermore, there are technological problems which do not allow fabrication of the efficient top GaInP junction of the *p*–*n* polarity [6].

Since MJ SCs include a large number of both nanodimensional (10–100 nm) and bulk (to 5 μm) layers of different chemical composition, multiple rereflection of light and interference phenomena occur in their structures, in contrast to single-junction SCs [7]. These phenomena have a significant effect on the spectral dependences of the photoresponse quantum efficiency (photoresponse spectral characteristics) of MJ SCs; therefore, simulating them faces the necessity of considering the complex propagation of electromagnetic waves in the structure. This makes it impossible to apply the classical methods for calculating the photoresponse spectral characteristics of single-junction structures to MJ SCs [8].

In [9, 10], we have demonstrated an analytical method for calculating the photoresponse spectral characteristics of MJ SCs, where the generation function was determined by formalizing the solution to the set of Maxwell's equations for a layered structure by the Abeles matrix method [11]. Carrier collection into the *p*–*n* junction was calculated by the diffusion model. The input parameters in the calculation were layer thicknesses, minority carrier (MC) diffusion lengths, recombination velocities at heterojunctions, and material properties. Since carrier propagation in thin layers (thinner than 50 nm) is almost independent of diffusion lengths [12], the contribution of thin layers of wide-gap “windows” or back surface field (BSF) to the photoresponse spectral characteristics was considered using the coefficients characterizing the fraction of carriers injected into the emitter and base, respectively, instead of the diffusion model.

In this paper, we present a technique for determining diffusion lengths in the layers of GaInP/GaInAs/Ge-based MJ SC and subcells composing them. The effect of the thickness of the *n*-GaInP nucleation layer on spectral characteristics of single-junction Ge SCs was studied, the dependences of diffusion lengths on the doping level for individual layers of an MJ SC structure were determined, and the effect of technological growth conditions on carrier diffusion lengths in layers of individual subcells of MJ SCs was analyzed.

2. EXPERIMENTAL TECHNIQUE AND SIMULATION

2.1. Photoconverter Samples

SC structures were grown by H-MOVPE at a reduced pressure. Metal–organic compounds were used as sources of Group-III elements (trimethylgallium (TMGa), trimethylaluminum (TMAI), and trimethylindium (TMIn)); arsine (AsH_3) and phosphine (PH_3) were used as sources of Group-V elements. The sources of *n*- and *p*-type dopants were silane (SiH_4) and diethylzinc (DEZn), respectively. Growth was performed on *p*-Ge (100) substrates misoriented by 6° in the (111) direction and on *n*- and *p*-GaAs (100) substrates misoriented by 2° in the (110) direction.

The front contact grid was fabricated by vacuum deposition through a mask formed by photolithography. After depositing the contact grid, the n^+ -GaAs contact layer was removed by chemical etching. Cells were separated using mesa etching. Two-layer ZnS/MgF₂ antireflective coatings (ARC) optimized for each structure were deposited on the sample surface.

The *n*–*p* Ge and *p*–*n* GaAs SCs with different base doping levels were fabricated. In this case, the doping level of the *p*-Ge substrate playing the role of base in the *n*–*p* Ge SC was varied from 3×10^{17} to $1 \times 10^{19} \text{ cm}^{-3}$; the doping level of the *n*-GaAs base was varied from 3×10^{16} to $2 \times 10^{17} \text{ cm}^{-3}$. The thickness of the *n*-GaInP nucleation layer playing the role of a wide-gap “window” for Ge samples was varied from 35 to 300 nm. The emitter and base thicknesses in *p*–*n* GaAs cells were 0.5 and 3 μm , respectively. AlGaAs alloys were used as BSF and wide-gap “window” layers. Three-junction *n*–*p* GaInP/GaInAs/Ge SCs and two-junction *n*–*p* GaAs/Ge and *n*–*p* GaInP/GaAs SCs were also fabricated.

2.2. Technique for Determining Diffusion Lengths

Using the technique of [9, 10] for fabricated the SC structures, photoresponse spectra were calculated. The absorptances and carrier diffusivities for cell materials and layer thicknesses were structural parameters. Thus, when the carrier generation function form is known, which can be determined by calculating the light-wave field in the MJ SC structure, the photoresponse spectral characteristics depend only on diffu-

Table 1. Electron diffusion lengths in *p*-Ge substrates at different doping levels, determined by approximating the Ge SC photoresponse spectra (Fig. 1)

$N_a, 10^{18} \text{ cm}^{-3}$	$L_n, \mu\text{m}$
0.3	100
5	10
10	2

sion lengths in photoactive layers and the surface recombination velocities at their interfaces.

However, in the general case, an increase in the recombination rate at heterojunctions can affect the photoresponse spectral characteristic shape, which is similar to that observed as MC diffusion lengths decrease. It can be shown that recombination rates at heterojunctions, exceeding 10^4 cm/s , affect the photoresponse spectra; in contrast, heterojunctions of most materials are characterized by values smaller than 10^4 cm/s [13], except for recombination rates on the surface of semiconductor materials.

Thus, at fixed recombination rates at heterojunctions, optimum estimates of MC diffusion lengths in the wide-gap “window,” emitter, base, and BSF, i.e., \hat{L}_{Win} , \hat{L}_{Em} , \hat{L}_{Base} , and \hat{L}_{BSF} can be found from the condition

$$\sum_{k=1}^N (Q_e^*(\lambda_k) - Q_e(\lambda, \hat{L}_{\text{Win}}, \hat{L}_{\text{Em}}, \hat{L}_{\text{Base}}, \hat{L}_{\text{BSF}}))^2 \quad (1)$$

$$= \min \left[\sum_{k=1}^N (Q_e^*(\lambda_k) - Q_e(\lambda, \mathbf{L}_{\text{Win}}, \mathbf{L}_{\text{Em}}, \mathbf{L}_{\text{Base}}, \mathbf{L}_{\text{BSF}}))^2 \right],$$

$$\lambda = [\lambda_1, \lambda_2, \dots, \lambda_N]^T, \quad (2)$$

where λ is the set of wavelengths for which the photoresponse is calculated; $Q_e^*(\lambda_k)$ is the experimentally measured photoresponse for the wavelength λ_k ; $Q_e(\lambda_k, L_{\text{Win}}, L_{\text{Em}}, L_{\text{Base}}, L_{\text{BSF}})$ is the calculated photoresponse for the wavelength λ_k and diffusion lengths L_{Win} , L_{Em} , L_{Base} , and L_{BSF} ; and \mathbf{L}_{Win} , \mathbf{L}_{Em} , \mathbf{L}_{Base} , and \mathbf{L}_{BSF} are the column vectors of MC diffusion lengths in the wide-gap “window,” emitter, base, and BSF, respectively, over which variations are performed.

3. RESULTS AND ANALYSIS

3.1. Diffusion Lengths of Minority Charge Carriers in the *p*-Ge and *n*-GaAs Layers

Figure 1 shows the spectra of the external quantum efficiency of the photoresponse of three *n*–*p* Ge SCs grown on *p*-Ge substrates with different doping levels and the results of their approximation. The layer thickness of the wide-gap *n*-GaInP “window” for all samples was 100 nm. The calculated diffusion lengths of cells in the *p*-Ge substrate are given in Table 1.

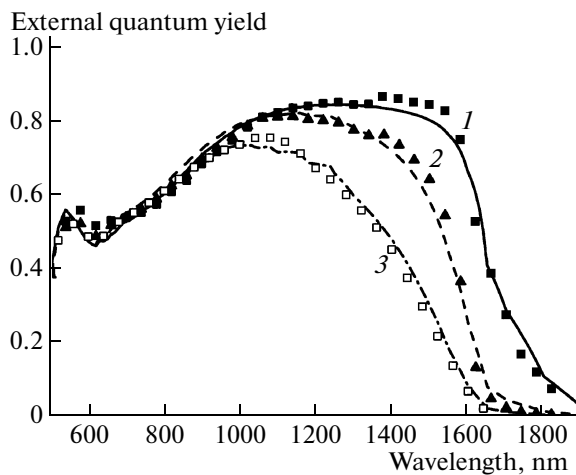


Fig. 1. Spectral dependences of the external quantum efficiency of the photoresponse to the photoactive surface for $n-p$ Ge SCs at p -Ge substrate doping levels $N_a = (1) 0.3$, (2) 5, and (3) $10 \times 10^{18} \text{ cm}^{-3}$. Solid curves and dots are the calculated and experimental values, respectively.

An increase in the substrate doping level resulted in a decrease in the long-wavelength photosensitivity of the studied SCs (Fig. 1), which was associated with a decrease in the electron diffusion length. At a level of $3 \times 10^{17} \text{ cm}^{-3}$, the electron diffusion length in p -Ge was $\sim 100 \mu\text{m}$, which allowed photogenerated carriers' collection close to the practical limit. Since an ARC was not deposited on the samples under study, the photoresponse efficiency did not exceed 85% (Fig. 1) due to the loss to incident radiation reflection from the cell surface.

Figure 2 shows the experimental and calculated data for $p-n$ GaAs SCs with different base doping levels. As in the case of Ge SCs, an increase in the doping level in the base layer of the n -GaAs SC resulted in a decrease in the hole diffusion length in it and a corresponding decrease in the long-wavelength sensitivity of the SC. The calculated MC diffusion lengths are given in Table 2. For the p -GaAs base layer, almost complete collection of carriers was provided at a doping level of $3 \times 10^{16} \text{ cm}^{-3}$.

3.2. Effect of p -GaInP Nucleation Layer Thickness on the Parameters of Single-Junction n - and p -Ge Cells

Figure 3 shows the experimental spectral characteristics of the photoresponse of $n-p$ Ge SCs with dif-

Table 2. Hole diffusion lengths in n -GaAs layers, determined by approximating the GaAs SC photoresponse spectra (Fig. 2)

$N_d, 10^{17} \text{ cm}^{-3}$	$L_p, \mu\text{m}$
0.3	10
1	7
2	3.5

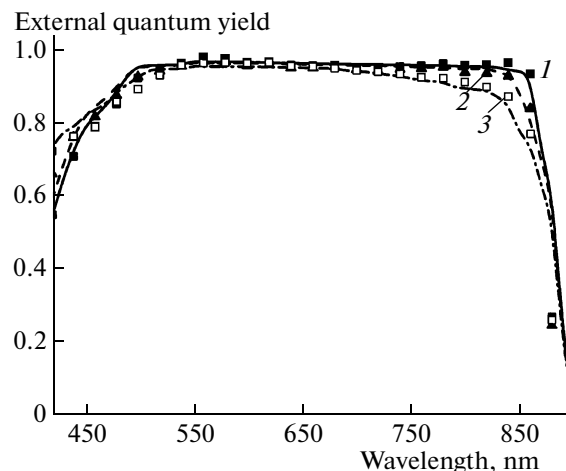


Fig. 2. Spectral dependences of the external quantum efficiency of the photoresponse to the photoactive surface for $p-n$ GaAs SCs at n -GaAs base layer doping levels $N_d = (1) 0.3$, (2) 1, and (3) $2 \times 10^{17} \text{ cm}^{-3}$. Solid curves and dots are the calculated and experimental values, respectively.

ferent thicknesses of the n -GaInP "window" and the results of their simulation. The p -Ge substrate doping level was $\sim 1 \times 10^{18} \text{ cm}^{-3}$ for all samples.

Approximation of spectral characteristics allowed the determination of MC diffusion lengths in n -GaInP wide-gap "window" layers (except for an SC with a window of 35 nm) and n -emitter and in the p -Ge substrate playing the role of a semi-infinite base (Table 3). The junction depth in cells was determined by secondary ion mass spectroscopy (SIMS) as $\sim 140 \text{ nm}$ for all samples. At an n -GaInP window thickness of 35 nm, its contribution was taken into account using the coefficient characterizing a fraction of carriers injected into the emitter, which probably reduced the accuracy of the estimate of the hole diffusion length in the n -Ge emitter (the injection probability was taken as 0.5).

The dependences of the photoresponse internal quantum yield of studied SCs (see the inset in Fig. 3) differed only in the spectral region of GaInP absorption (the wavelength region to 700 nm); the calculated MC diffusion lengths in n -GaInP wide-gap "window" layers, n -Ge emitter, and p -Ge base were almost completely identical for different cells (Table 3). This allows the conclusion that the decrease in the short-wavelength photosensitivity is associated only with the loss of carriers absorbed in the wide-gap n -GaInP "window." These losses are accounted for by the small hole diffusion length ($0.1 \mu\text{m}$) in the "window" layer.

Thus, the simulation in this case allowed us, without direct measurements, to conclude that the depth and distribution profile of phosphorus atoms in Ge were identical for the studied samples with different n -GaInP layer thicknesses. It should be noted that the

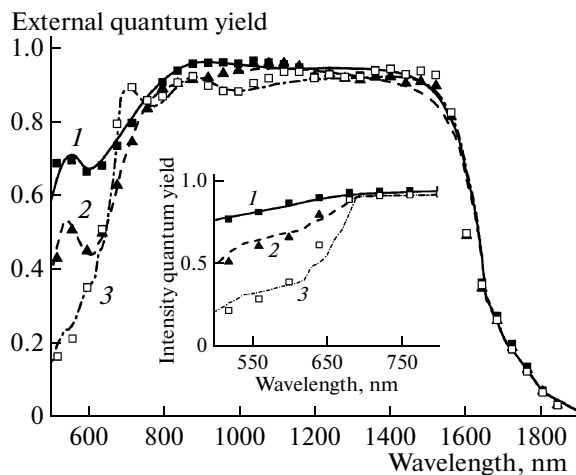


Fig. 3. Spectral dependences of the external quantum efficiency of the photoresponse to the photoactive surface for $n-p$ Ge SCs at nucleation n -GaInP layer thicknesses of (1) 35, (2) 100, and (3) 300 nm. Solid curves and dots are the calculated and experimental values, respectively. The inset shows the dependences of the internal quantum yield of the photoresponse for these SCs.

hole diffusion length in the Ge SC emitter appeared to be twice as large as its thickness, which created conditions for almost complete carrier collection from it and provided a close to 100% external quantum yield of the photoresponse almost in the entire spectral range of the photosensitivity of such SCs, except for the range of 500–700 nm.

3.3. Characteristics of GaAs and Ge Cells in Multijunction MJ SCs

Three-junction $n-p$ GaInP/GaInAs/Ge MJ SCs were grown retaining the fabrication technology of the bottom diffusion subcell. However, growth of the two-junction GaInP/GaInAs structure on the Ge subcell resulted in a significant change in its photoresponse spectra (Fig. 4).

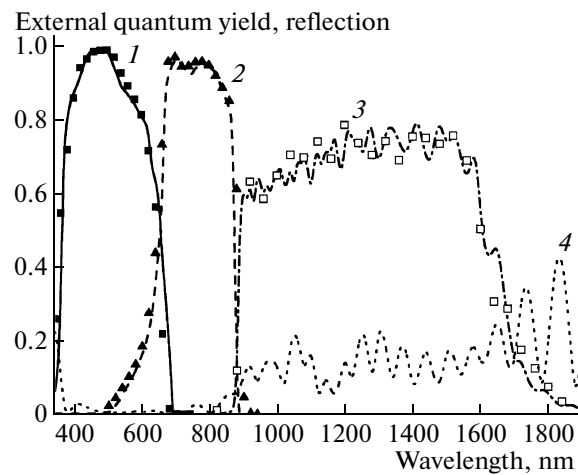


Fig. 4. Spectral dependences of the external quantum efficiency of the photoresponse to the photoactive surface for the (1) GaInP subcell, (2) GaInAs subcell, (3) Ge subcell of the GaInP/GaInAs/Ge MJ SC, and (4) reflection from the structure. Curves 1–3 and dots are the calculated and experimental values, respectively.

The wavy shape of the photoresponse spectral characteristic of Ge subcells, in contrast to the case of single-junction Ge SCs, was associated with interference phenomena in the multilayer MJ SC structure; narrowing of the sensitivity range with absorption of photons with wavelengths >900 nm was associated with interference phenomena in the top subcells.

Furthermore, the photoresponse level of Ge subcells of GaInP/GaInAs/Ge SCs was significantly lower than that of single-junction Ge SCs. This was in part caused by reflection from the structure surface in the range of 900–1900 nm, which was about 10–15% (Fig. 4). However, the photoresponse internal quantum yield of the Ge subcell of MJ SCs did not exceed 80% and exhibited an obvious decrease in the short-wavelength region. This was associated with deeper diffusion of phosphorus atoms into the p -Ge substrate in the case of long-term growth of the cascade struc-

Table 3. Parameters of the calculation of the external and internal quantum efficiencies of the photoresponse of Ge SCs with different thicknesses of the wide-gap n -GaInP “window” layer (Fig. 3)

Thickness of the n -GaInP “window”, nm	n -Ge	p -Ge	n -GaInP	n -Ge	p -Ge	n -GaInP	n -Ge	p -Ge
	35		100		300			
L_p , μm	0.35		0.1	0.3		0.1	0.3	
L_n , μm		50			50			50
D_p , cm^2/s	30		5	30		5	30	
D_n , cm^2/s		80			80			80
S , cm/s	$<10^4$	∞	$\sim 10^5$	$<10^4$	∞	$\sim 10^5$	$<10^4$	∞

Note: For n -layers (emitter), S means the recombination rate at the heterojunction with the wide-gap “window”; for p -layers (base), it is the recombination rate at the interface with the back metal contact; for wide-gap “window” layers, S is the surface recombination rate.

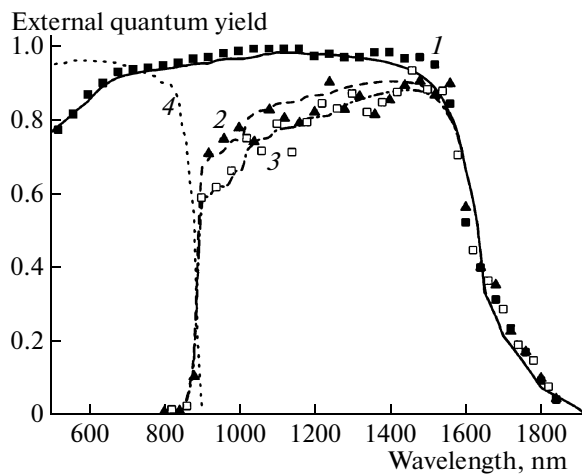


Fig. 5. Spectral dependences of the internal quantum efficiency of the photoresponse to the photoactive surface for Ge junctions: (1) single-junction Ge SC, (2) two-junction GaAs/Ge MJ SC, (3) three-junction GaInP/GaInAs/Ge MJ SC, and (4) the photoresponse spectral characteristic edge for the GaInAs subcell in the MJ SC. Curves 1–3 and dots are the calculated and experimental values, respectively.

ture. According to the SIMS data, the diffusion depth in three-junction GaInP/GaInAs/Ge SCs was ~ 700 nm.

Figure 5 compares the photoresponse internal quantum yield of single-junction Ge SCs and bottom Ge subcells of two-junction GaAs/Ge and three-junction GaInP/GaInAs/Ge SCs. The structures were grown on identical substrates under identical epitaxial growth conditions.

The diffusion lengths at which the best agreement between calculated and experimental data for the single-junction Ge SC and the Ge subcell of the three-junction GaInP/GaInAs/Ge SC appeared identical (Table 4). Simulation of the spectral characteristic of the Ge subcell of GaAs/Ge MJ SCs at the same diffusion lengths allowed us to determine the $p-n$ junction depth as ~ 500 nm (Table 4).

Spectral characteristics of the photoresponse of the single-junction $n-p$ GaAs SC, Ga(In)As subelements of two-junction GaInP/GaAs and three-junction GaInP/GaInAs/Ge SCs are shown in Fig. 6. The calculation parameters providing the best agreement

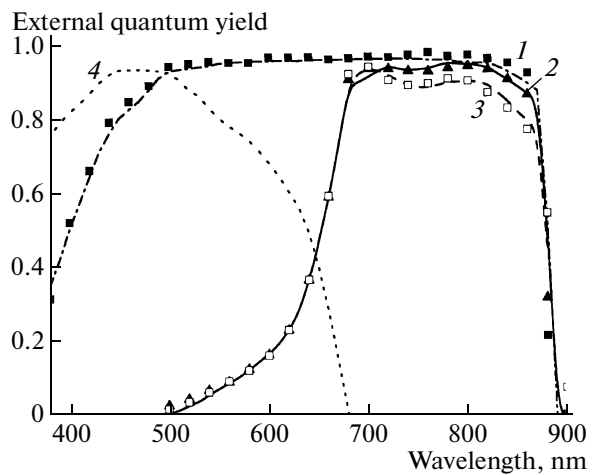


Fig. 6. Spectral dependences of the external quantum efficiency of the photoresponse to the photoactive surface for GaAs junctions: (1) single-junction Ga(In)As SC, (2) two-junction GaInP/GaAs SC, (3) three-junction GaInP/GaAs/Ge SC, and (4) the photoresponse spectral characteristic for the GaInP subcell in the MJ SC. Curves 1–3 and dots are the calculated and experimental values, respectively.

between calculated and experimental characteristics shown in Fig. 6 are listed in Table 5.

An increase in the number of subcells in MJ SCs while retaining the epitaxial growth conditions resulted in a decrease in MC diffusion lengths in Ga(In)As subcell layers. The wavy shape of the characteristics of two- and three-junction cells was caused by interference in the top GaInP subcell and tunnel junction layers. The general level lowered due to a decrease in MC diffusion lengths and absorption of a useful radiation fraction in tunnel junction layers.

Hole diffusion lengths in n -Ga(In)As emitters for MJ SCs were shorter in comparison with single-junction SCs (Table 5). This was most likely due to p -impurity diffusion from structure top layers.

Single-junction GaAs SCs and the bottom subcell of two-junction GaInP/GaAs MJ SCs were grown by similar technology on identical substrates; therefore, electron diffusion lengths in bases of such cells differed insignificantly. The small electron diffusion length observed in the p -GaInAs base of the three-junction MJ SC based on GaInP/GaInAs/Ge was probably

Table 4. Diffusion lengths and junction depths for the layers composing Ge cells the photoresponse spectra of which are shown in Fig. 5

	Junction depth, nm	L_p , μm	L_n , μm
Single-junction Ge cell	140	0.4	50
Two-junction GaAs/Ge SC	500*	0.4	50
Three-junction GaInP/GaInAs/Ge SC	700	0.4	50

Note: * is the calculated value.

Table 5. Diffusion lengths for Ga(In)As subcells of MJ SCs shown in Fig. 6

	L_p , μm	L_n , μm
Single-junction GaAs cell	0.5	10
Two-junction GaInP/GaAs SC	0.3	8
Three-junction GaInP/GaInAs/Ge SC	0.3	4

caused by lowering of the structural quality of GaInAs layers during III–V structure growth on germanium substrates.

4. CONCLUSIONS

Thus, the applicability of numerical simulation to the analysis of the parameters of layers composing MJ SC structures was demonstrated. The advantage of this approach is the possibility of estimating MC diffusion lengths in SC layers in the simulation of their photoresponse spectral characteristics without additional measurements. The approximation of the photoresponse spectra made it possible to determine the dependences of MC diffusion lengths in p -Ge and n -GaAs layers on their doping level and to determine the values at which complete carrier collection from base layers of $n-p$ Ge and $p-n$ GaAs SCs was provided. An analysis of the simulation data allowed the conclusion to be drawn that the decrease in the short-wavelength region of photoresponse spectra of $n-p$ Ge SCs with increasing the n -GaInP layer thicknesses was associated with the loss of photons absorbed in this layer, rather than with the change in the diffusion $p-n$ junction parameters. A decrease in the diffusion length in Ga(In)As layers of subcells and an increase in the $p-n$ junction depth in the Ge substrate with the number of MJ SC junctions were detected.

ACKNOWLEDGMENTS

We are grateful to S.I. Troshkov for helpful discussions and B.Ya. Ber, A.P. Koval'skii, and D.Yu. Kazantsev for SIMS measurements.

This study was supported by the Russian Foundation for Basic Research, projects nos. 08-08-00916-a, 09-08-00879-a, and 09-08-00954-a.

REFERENCES

1. T. Markwart and L. Castaner, *Solar Cells: Materials, Manufacture and Operation* (Elsevier Sci., Amsterdam, 2005).
2. W. Guter, J. Schöne, S. P. Philipps, M. Steiner, G. Siefer, A. Wekkeli, E. Weiser, E. Oliva, A. W. Bett, and F. Dimroth, *Appl. Phys. Lett.* **94**, 223504 (2009).
3. M. Meusel et al., in *Proc. of the 20th EPSEC* (Barcelona, Spain, 2005), p. 20.
4. L. M. Fraas, J. E. Avery, H. X. Huang, E. Shifman, K. Edmondson, and R. R. King, in *Proc. of the 31th PVSC* (Florida, USA, 2005), p. 751.
5. M. Z. Shvarts, P. Y. Gazaryan, N. A. Kaluzhnii, V. P. Khvostikov, V. M. Lantratov, S. A. Mintairov, S. V. Sorokina, and N. K. Timoshina, in *Proc. of the 21st EPSEC* (Dresden, Germany, 2006), p. 133.
6. A. S. Gudovskikh, N. A. Kaluzhnii, V. M. Lantratov, S. A. Mintairov, M. Z. Shvarts, and V. M. Andreev, *Thin Sol. Films* **516**, 6739 (2008).
7. M. Born and E. Wolf, *Principles of Optics*, 7th ed. (Cambridge Univ., UK, 2002).
8. A. M. Vasil'ev and A. P. Landsman, *Semiconductor Photocurrents* (Sov. radio, Moscow, 1971) [in Russian].
9. V. M. Emel'yanov, N. A. Kalyuzhnii, S. A. Mintairov, and V. M. Lantratov, *NTV SPbGU* **2**, 17 (2009).
10. V. M. Andreev, V. M. Emelyanov, N. A. Kalyuzhnii, V. M. Lantratov, S. A. Mintairov, M. Z. Shvarts, and N. K. Timoshina, in *Proc. of the 23th EPSEC* (Valencia, Spain, 2008), p. 375.
11. F. Abeles, *Ann. Phys.* **45**, 596 (1950).
12. V. B. Egorov, Extended Abstract of Candidate's Dissertation (Fiz. Tekh. Inst., Leningrad, 1986).
13. Yu. A. Goldbery, *Handbook Series on Semiconductor Parameters*, Ed. by M. Levinshtein, S. Rumyantsev, and M. Shur (World Sci., London, 1996), vol. 1.

Translated by A. Kazantsev